cancers

MDPI

Article

CYP1B1: A Novel Molecular Biomarker Predicts Molecular Subtype, Tumor Microenvironment, and Immune Response in 33 Cancers

Benchao Yuan [1,†], Guihong Liu [2,†], Zili Dai [3], Li Wang [3], Baisheng Lin [3] and Jian Zhang [3,4,*]

[1] Department of Oncology and Hematology, The Sixth People's Hospital of Huizhou City, Huiyang Hospital Affiliated to Southern Medical University, Huizhou 516003, China
[2] Department of Radiation Oncology, Dongguan Tungwah Hospital, Dongguan 523120, China
[3] Department of Radiation Oncology, Affiliated Cancer Hospital & Institute of Guangzhou Medical University, State Key Laboratory of Respiratory Diseases, Guangzhou Institute of Respiratory Disease, Guangzhou 510095, China
[4] Guangzhou Medical University, Guangzhou 511495, China
* Correspondence: zhangjian@gzhmu.edu.cn; Tel./Fax: +86-020-66673666
† These authors contributed equally to this work.

Simple Summary: Cytochrome P450 Family 1 Subfamily B Member 1 (CYP1B1) is a critical metabolic enzyme of melatonin. Although melatonin has been identified to exhibit tumor suppressing activity, the role and mechanism of the clinical and immunological characteristics of CYP1B1 in cancer remain unclear. We comprehensively explored the clinical and immunological characteristics of CYP1B1. We identified that the dysregulated expression of CYP1B1 was associated with clinical characteristics and a tumor immune microenvironment, which may provide a promising predictor and molecular target for clinical immune treatment.

Abstract: Background: Cytochrome P450 Family 1 Subfamily B Member 1 (CYP1B1) is a critical metabolic enzyme of melatonin. Although melatonin has been identified to exhibit tumor suppressing activity, the role and mechanism of the clinical and immunological characteristics of CYP1B1 in cancer remain unclear. Methods: In this study, RNA expression and clinical data were obtained from The Cancer Genome Atlas (TCGA) across 33 solid tumors. The expression, survival, immune subtype, molecular subtype, tumor mutation burden (TMB), microsatellite instability (MSI), biological pathways, and function in vitro and vivo were evaluated. The predictive value of CYP1B1 in immune cohorts was further explored. Results: We found the dysregulated expression of CYP1B1 was associated with the clinical stage and tumor grade. Immunological correlation analysis showed CYP1B1 was positively correlated with the infiltration of lymphocyte, immunomodulator, chemokine, receptor, and cancer-associated fibroblasts (CAFs) in most cancer. Meanwhile, CYP1B1 was involved in immune subtype and molecular subtype, and was connected with TMB, MSI, neoantigen, the activation of multiple melatonergic and immune-related pathways, and therapeutic resistance. Conclusions: Together, this study comprehensively revealed the role and mechanism of CYP1B1 and explored the significant association between CYP1B1 expression and immune activity. These findings provide a promising predictor and molecular target for clinical immune treatment.

Keywords: pan-cancer; CYP1B1; tumor mutation burden; microsatellite instability; neoantigen; immune activity

Citation: Yuan, B.; Liu, G.; Dai, Z.; Wang, L.; Lin, B.; Zhang, J. CYP1B1: A Novel Molecular Biomarker Predicts Molecular Subtype, Tumor Microenvironment, and Immune Response in 33 Cancers. *Cancers* **2022**, *14*, 5641. https://doi.org/10.3390/cancers14225641

Academic Editor: J. Chad Brenner

Received: 14 October 2022
Accepted: 16 November 2022
Published: 17 November 2022

1. Introduction

Melatonin, an endogenous hormone, is secreted by the pineal gland in response to biological rhythm [1,2]. The synthesis and metabolism of the hormone involves a series of biological pathways. In the process of melatonin synthesis, N-acetylserotonin

(NAS) was firstly combined to serotonin by arylalkylamine N-acetyltransferase (AANAT) and methylated by acetylserotonin O-methyltransferase (ASMT) [3]. The melatonin is further metabolized into 6-hydroxymelatonin (6OH-MEL) by human cytochrome P450 family [4]. Evidence shows that various biological properties of melatonin, such as the circadian clock [5–7], sleep regulation [8,9], anti-inflammatory properties [10–12], immune modulation [13–15], and anti-cancer activities [16–18], have been well revealed. Nevertheless, the clinical and immunological function of the cytochrome P450 family in cancer remains unclear.

Cytochrome P450 1B1 (CYP1B1), one member of the cytochrome P450 family, is an extrahepatic enzyme that is involved in the metabolism of melatonin [4] and other compounds [19–22]. The exogenous carcinogens, such as aromatic amines and polycyclic aromatic hydrocarbons, can be oxidized by CYP1B1 to active carcinogenic products. Accumulated evidence has revealed that the single nucleotide polymorphism of CYP1B1 is associated with the risk of cancer, including prostate, endometrial, and ovarian cancer [23–25]. Recent studies have also linked CYP1B1 expression to clinical grade lymphovascular invasion and lymph node metastasis [26,27]. CYP1B1 is also involved in the positive regulation of inflammatory cytokine, which acts on both cancer cells and the tumor microenvironment [28]. However, the role and mechanism of CYP1B1 in the immune microenvironment still remains to be demonstrated.

In this study, we investigated the clinical and immunological aspects of the metabolic enzyme CYP1B1 among 33 solid tumors from The Cancer Genome Atlas (TCGA) databases. We identified that the dysregulated expression of CYP1B1 was associated with clinical stage, grade, and survival. CYP1B1 was involved in the infiltration of the lymphocyte, immunomodulator, chemokine, receptor, and cancer associated fibroblast (CAF) in cancer. Furthermore, we also probed insight into the immune subtype, molecular subtype, tumor mutation burden (TMB), microsatellite instability (MSI), neoantigen, and immune-related pathways mediated by CYP1B1, which may provide a promising predictor and molecular target for clinical immune treatment.

2. Materials and Methods

2.1. Data Collection

The expression, phenotype, and survival data were obtained from the UCSC Xena database (https://xenabrowser.net/, accessed on 22 May 2020). The lymphocyte, immunomodulator, chemokine, immune subtype, and molecular subtype were downloaded from the Tumor-Immune System Interactions (TISIDB) database (http://cis.hku.hk/TISIDB/index.php, accessed on 23 March 2019). The cancer-associated fibroblasts (CAFs) data were obtained from TIMER 2.0 (http://timer.cistrome.org/, accessed on 2 July 2020). The TCGA database was used to obtain the tumor mutation burden (TMB), microsatellite instability (MSI), and neoantigen. The study was conducted in accordance with the Declaration of Helsinki (as revised in 2013) and was approved by the Ethics Committee of The Sixth People's Hospital of Huizhou City (PJ2022MI-KJ038).

2.2. Differential Gene Expression Analysis

To identify the expression differences of CYP1B1 between tumor samples and normal tissues, the expression data of 33 cancers was downloaded from the UCSC Xena database. The expression values were normalized by Transcripts Per Million (TPM) transformation. A distinction with a threshold of $p < 0.05$ was considered as having a significance.

2.3. Survival Analysis

The KM-plotter analysis of 33 cancer patients were examined using univariate COX regression analysis to determine the prognostic significance of CYP1B1. The forest plot was performed using the R software forest plot package. A log-rank test with a threshold of $p < 0.05$ was considered as having a significance.

2.4. Correlation Analysis between CYP1B1 and Tumor Immune System

To clarify the relation between CYP1B1 and the tumor immune system, the potential relationship among CYP1B1 and 28 lymphocytes, 69 immunomodulators (45 immunostimulators, 24 immunoinhibitors), 41 chemokines, and 18 receptors, immune subtypes and molecular subtypes were explored using the TISIDB database. The relationship of CYP1B1 and CAF was assessed by the TIMER 2.0 database. The correlation of CYP1B1 and TMB, MSI, and neoantigen were further evaluated. $p < 0.05$ was considered as having a significance.

2.5. Single-Sample Gene Set Enrichment Analysis (ssGSEA)

To identify the CYP1B1 activity in cancer, the single sample gene sets enrichment analysis (ssGSEA) between high CYP1B1 and low CYP1B1 expression was evaluated by using R software GSVA package. $p < 0.05$ was considered as having a significance.

2.6. Association between CYP1B1 and Drug Response

CCLE gene expression data were quantile normalized among all different cell lines for partial correlation, and then Z-score normalization was applied in each tissue to calculate the expression difference between High–Low (using the median as a cutoff) IC50 groups. The X-axis indicates the mean/median expression difference across tissues. Correlations of CYP1B1–drug associations after controlling for the tissue average expression were analyzed.

2.7. Gene Set Enrichment Analysis (GSEA)

Correlations with other genes and ordered genes based on findings were performed to discover the biological aspects of CYP1B1. The sorted gene list was used in GSEA analysis to see if highly linked genes clustered in genuinely functional pathways. The reference gene set was annotated gene set c5.go.v7.4.symbols.gmt and c2.cp.kegg.v7.4.symbols.gmt. As previously stated, FDRs of 0.05 and p-values of 0.01 were considered significant.

2.8. Cell Culture

The lung cancer cell line PC9, breast cancer cell lines MDA-MB-231 was obtained from the Sun Yat-sen University Cancer Center. Cells were maintained at 37°, 5% CO_2 in 10% DMEM (Invitrogen, Carlsbad, CA, USA) or RPMI-1640 (Thermo Fisher Scientific, Waltham, MA, USA) supplemented with 10% fetal bovine serum.

2.9. Wound Healing Assay

Cells were cultured in 10% DMEM (Invitrogen, Carlsbad, CA, USA) or RPMI-1640 (Gibco, Australia), supplemented with 10% fetal bovine serum at 37°, 5% CO_2. The medium was removed, and the surface of the inoculated cells was scratched and marked with a 10 µL pipette tip. A sterile 200-L pipette tip was used to scrape the surface of the cell monolayer to create the wound. Under an inverted microscope, photographs were taken at time 0 and 24 h after cell scratching (Olympus Corporation). The area of each wound was calculated using Image J software (National Institutes of Health).

2.10. Transwell Assay

Transwell plates (8-m pores) were used for Transwell migration or invasion studies. Next, 5×10^4 (migration assay) or 1×10^5 (invasion assay) cells resuspended in serum-free medium were placed in the top chamber, either uncoated or covered with Matrigel (BD Biosciences). The culture medium in the lower compartment included 10% FBS. The cells were fixed and stained after being incubated for 12 or 24 h. Cells on the undersides of the filters were seen and counted at a magnification of 200 magnification.

2.11. Cell Proliferation Assay

The cancer cell line was seeded in 1000 cells per plate and cultured for two weeks at 37 °C in a 5% CO_2 incubator. The cells were washed twice, fixed for 15 min with 4%

paraformaldehyde, then stained for 20 min at room temperature with 1% crystal violet solution. The number of visible colonies was determined.

2.12. In Vivo Metastasis Model

The Guangzhou Medical University Cancer Center's Institutional Animal Care and Use Committee authorized the animal operations (Guangzhou, China, G2022-050). First, 1×10^7 PC9 cells were injected into the footpads of mice for the tumor metastasis model. After 2 weeks, the mice were euthanized, and their footpad tumors and inguinal lymph nodes were removed after being intraperitoneally administered with melatonin (25 mg/kg) every other day for 7 consecutive days.

2.13. Immunohistochemistry Analysis

The deparaffinized sections were incubated with 5% normal goat serum (Beyotime, Shanghai, China) to block endogenous peroxidase activity, then the tumor sections were incubated with the primary anti-CYP1B1 (Proteintech, Wuhan, China, 18505-1-AP, 1:200), anti-CD31 (Abcam, Cambridge, UK, ab182981, 1:2000), Ki67 (Abcam, ab16667, 1:400), LY6G (Abcam, ab238132, 1:1000), MMP9 (Boster, Wuhan, China, PB9669, 1:200) antibody at 4 °C overnight. After incubation with the secondary antibody, the staining was visualized using the DAKO REAL EnVision Inspection System (DAKO).

2.14. Statistical Analysis

All statistical analyses were performed using R software (version 4.0.3). The correlations between CYP1B1 and clinicopathological features were detected by Chi square test. Univariate analysis was used to estimate the prognostic value of CYP1B1. The correlation analysis was assessed by the Spearman rank test. $p < 0.05$ was considered statistically significant.

3. Results

3.1. The Expression, Tumor Stage and Clinical Grade of CYP1B1 in Cancer

By investigating RNA-seq data from 33 cancers in the TCGA, we explored the differential expression of CYP1B1 between tumor samples and healthy samples. As shown in Figure 1A, CYP1B1 was significantly downregulated in most of the cancers.

The relationship between CYP1B1 expression and clinical prognosis in 33 cancers was further analyzed. According to the median expression of CYP1B1, the cancers were divided into high- and low-expression groups. CYP1B1 was associated with protective overall survival (OS) in SKCM and SARC, and risky OS in STAD, KIRC, and BLCA (Figure S1A). Similarly, CYP1B1 was associated with protective disease-specific survival (DSS) in THYM and disease free interval (DFI) in LGG (Figure S1B,C). CYP1B1 was associated with risky DSS in BLCA, COAD, KIRC, KIRP and STAD, DFI in OV and STAD, and progression free interval (PFI) in GBM, KIRC, and STAD (Figure S1B–D). The associations between CYP1B1 and the clinical stage showed that a higher expression of CYP1B1 was positively related to the tumor stage in BLCA (r = 0.218, $p = 9.21 \times 10^{-6}$; Figure 1B), KIRC (r = 0.139, $p = 0.00129$; Figure 1C), SKCM (r = 0.144, $p = 0.00354$; Figure 1D), STAD (r = 0.123, $p = 0.0146$; Figure 1E), THCA (r = 0.094, $p = 0.0364$; Figure 1F), and UCEC (r = 0.177, $p = 0.00898$; Figure 1G). The associations in the tumor grade found that the lymphocyte, immunomodulator, chemokine, and receptor were positively related to the tumor grade in HNSC (r = 0.187, $p = 2.64 \times 10^{-5}$; Figure 1H), KIRC (r = 0.215, $p = 6.98 \times 10^{-7}$; Figure 1I), STAD (r = 0.123, $p = 0.0146$; Figure 1J), and negatively related with grade in LIHC (r = –0.159, $p = 0.00224$; Figure S2). These findings suggested that dysregulated CYP1B1 expression might serve as a predictive biomarker for cancer.

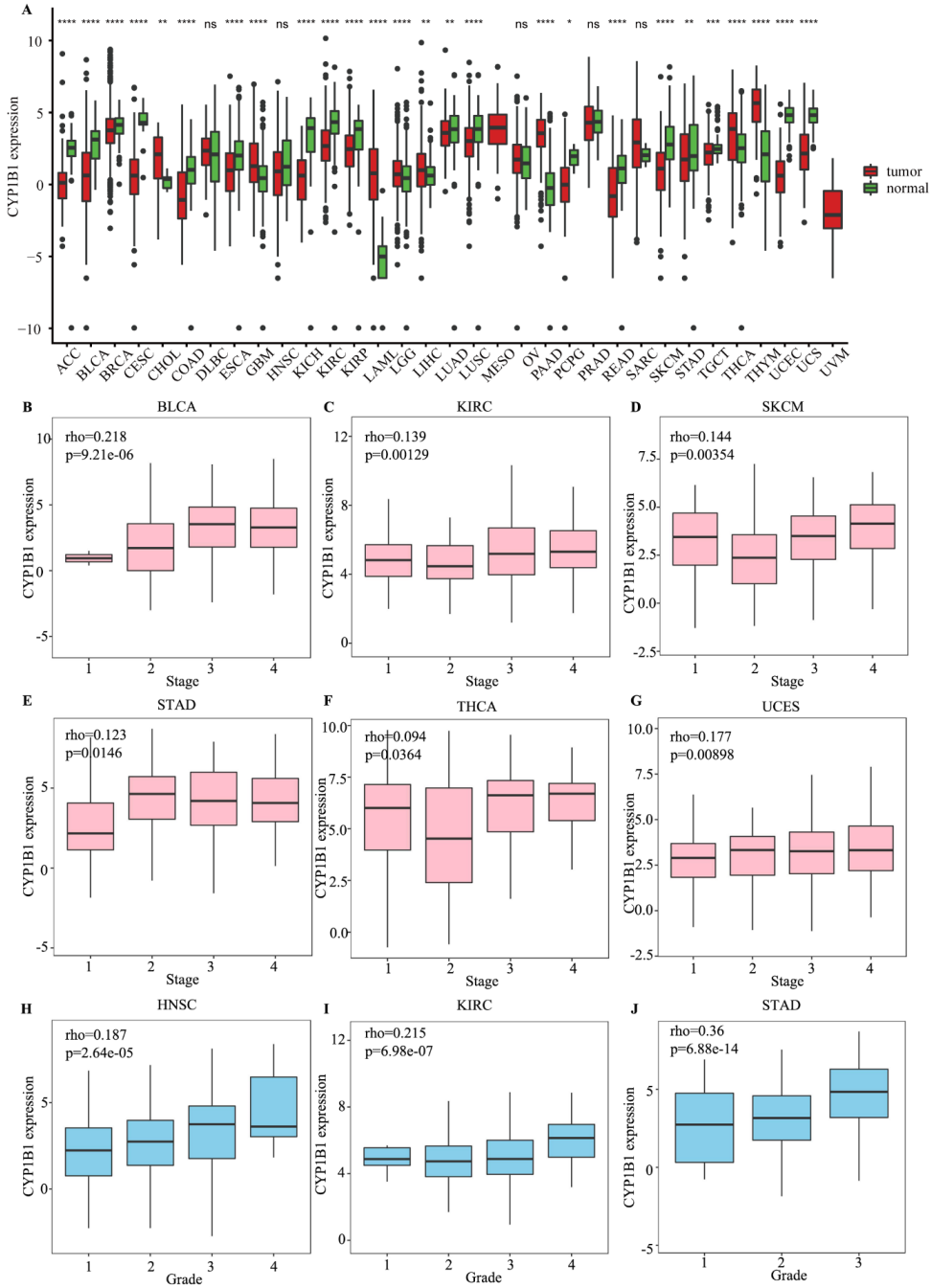

Figure 1. CYP1B1 expression, stage and grade in cancer. (**A**) CYP1B1 expression between tumor and normal samples in cancer. (**B**–**G**) The positive correlation between CYP1B1 expression and clinical stage in in BLCA (**B**), KIRC (**C**), SKCM (**D**), STAD (**E**), THCA, (**F**) and UCEC (**G**). (**H**–**J**) The positive correlation between CYP1B1 expression and tumor grade in HNSC (**H**), KIRC (**I**), and STAD (**J**). * means $p < 0.05$; ** means $p < 0.01$; *** means $p < 0.001$; **** means $p < 0.0001$; *ns* means no significance.

3.2. The Correlation among CYP1B1 Expression and Lymphocyte, Immunomodulator, Chemokine and Receptor

To identify the function of CYP1B1 expression in immune regulation, CYP1B1 expression was positively associated with lymphocyte and MHC molecule in most cancer. As shown in Figure 2A, CYP1B1 was positively related to Tem CD8 cell (r = 0.644, $p = 3.43 \times 10^{-5}$) and NKT cell (r = 0.71, $p = 2.86 \times 10^{-6}$) in CHOL and negatively related to act CD8 cell (r = −0.241, $p = 0.0706$) and CD56 bright (r = −0.252, $p = 0.059$) in UCS. Regarding the MHC molecule, CYP1B1 was also positively related to HLA-DOA expression

(r = 0.463, p = 0.00485) and HLA-DRA expression (r = 0.544, p = 0.000734) in CHOL, and negatively related to HLA-DOA expression (r = −0.22, p = 0.0994) and HLA-G expression (r = −0.248, p = 0.0633) in UCS (Figure 2B).

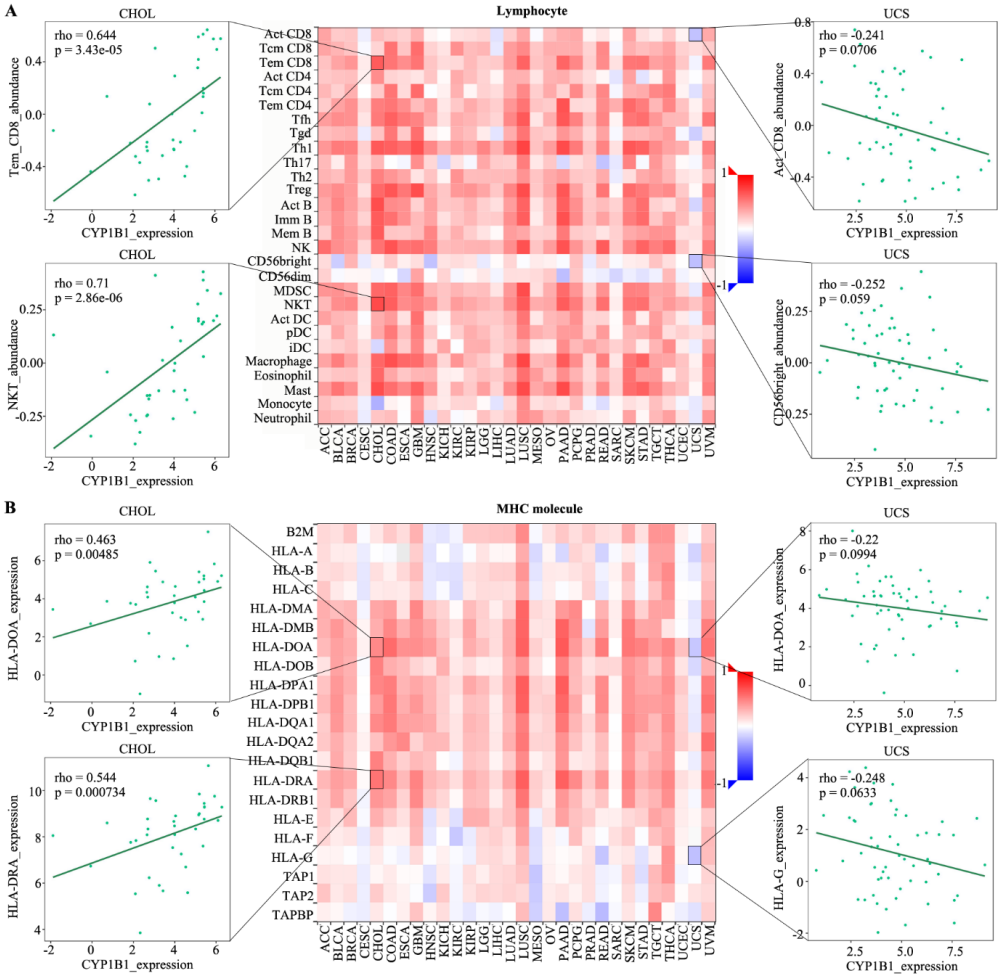

Figure 2. The correlations between CYP1B1 expression and lymphocyte and MHC molecule. (**A**) The spearman correlations between CYP1B1 expression and lymphocyte in cancer. (**B**) The spearman correlations between CYP1B1 expression and MHC molecule in cancer. The heatmap represents rho value. Red color means positive correlation, blue color means negative correlation. Four associations were showed by dot plots.

Next, the role of CYP1B1 in the immunostimulator was further evaluated. As depicted in Figure S3A, CYP1B1 was positively related to CD40LG expression (r = 0.677, $p = 1.0 \times 10^{-5}$) and TNFSF13B expression (r = 0.536, $p = 9.08 \times 10^{-4}$) in CHOL and negatively related to act CD27 expression (r = −0.337, p = 0.0106) and KLRK1 expression (r = −0.274, p = 0.0392) in UCS. Further, regarding immunoinhibitor, CYP1B1 was positively associated with BTLA expression (r = 0.66, $p = 1.94 \times 10^{-5}$) and PDCD1LG2 expression (r = 0.628, $p = 6.11 \times 10^{-5}$) in CHOL and negatively associated with act CD160 expression (r = −0.273, p = 0.0402) and LAG expression (r = −0.294, p = 0.0268) in UCS (Figure S3B).

In addition, considering the chemokine, CYP1B1 was positively associated with CCL14 expression (r = 0.659, $p = 1.98 \times 10^{-5}$) and CCL19 expression (r = 0.75, $p = 7.51 \times 10^{-7}$) in CHOL and negatively associated with act CCL20 expression in UCS (r = −0.396, $p < 2.2 \times 10^{-16}$) and CXCL1 expression (r = −0.424, $p < 2.2 \times 10^{-16}$) in STAD (Figure S4A); regarding the receptor, CYP1B1 was positively associated with CCR4 expression (r = 0.719, $p = 2.03 \times 10^{-6}$) and CXCR4 expression (r = 0.618, $p = 8.53 \times 10^{-5}$) in CHOL and negatively

associated with act CCR6 expression in READ (r = −0.259, $p = 7.46 \times 10^{-4}$) and CCR9 expression (r = −0.461, $p = 1.15 \times 10^{-4}$) in KICH (Figure S4B).

3.3. Correlation between CYP1B1 and CAFs in the Tumor Microenvironment

CAFs, the most abundant stromal cells in the tumor microenvironment (TME), are associated with tumor cell growth, invasion, and metastasis, metabolic reprograming, immune escape, and therapeutic resistance [29–31]. Four algorithms, including EPIC, MCPCOUNTER, XCELL, and TIDE, were used to evaluate the correlation between the CAFs and the CYP1B1 expression level in 33 cancers. Cancers with consistent correlations of four algorithms were considered to be importantly associated with CAFs infiltration. As shown in Figure 3A, the expression of CYP1B1 was importantly positively correlated with CAFs infiltration in BLCA, BRCA, BRCA-LumA, CESC, CHOL, COAD, ESCA, GBM, HNSC, HNSC-HPV-, HNSC-HPV+, KIRC, KIRP, LIHC, LUAD, LUSC, MESO, PAAD, PCPG, READ, SKCM, SKCM-Metastasis, STAD, TGCT, THYM, and UCEC. The correlation estimated by the EPIC, MCPCOUNTER, XCELL, and TIDE algorithms were displayed as examples in Figure 3. For example, the expression of CYP1B1 was positively correlated with the level of infiltration of CAFs in BRCA (r = 0.398, $p = 1.95 \times 10^{-15}$; r = 0.39, $p = 7.98 \times 10^{-15}$; r = 0.321, $p = 2.78 \times 10^{-10}$; r = 0.353, $p = 3.12 \times 10^{-12}$; Figure 3B–E) and SKCM-Metastasis (r = 0.59, $p = 1.43 \times 10^{-34}$; r = 0.56, $p = 1.41 \times 10^{-30}$; r = 0.199, $p = 1.69 \times 10^{-4}$; r = 0.467, $p = 1.47 \times 10^{-20}$; Figure 3F–I). These results indicated that CAFs infiltration mediated by CYP1B1 were critical for cancer occurrence and progression in the TME.

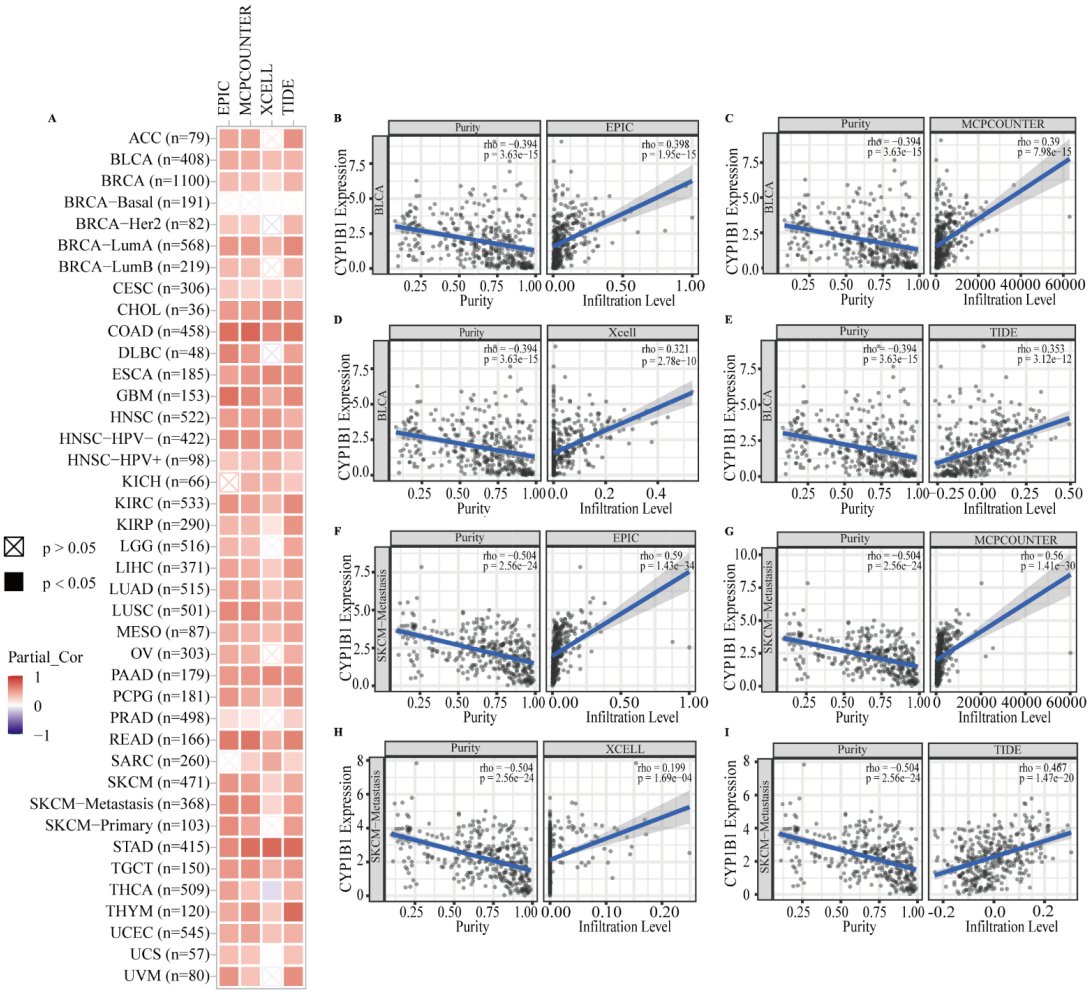

Figure 3. The correlations between CYP1B1 expression and immune infiltration of cancer-associated fibroblasts. (**A**) The correlation between CYP1B1 expression and CAFs infiltration estimated by the

EPIC, MCPCOUNTER, XCELL, and TIDE algorithm in cancer. (**B**–**E**) The correlation between CYP1B1 expression and CAFs infiltration estimated by the EPIC (**B**), MCPCOUNTER (**C**), XCELL (**D**), and TIDE (**E**) algorithm in BRCA. (**F**–**I**) The correlation between CYP1B1 expression and CAFs infiltration estimated by the EPIC (**F**), MCPCOUNTER (**G**), XCELL (**H**), and TIDE (**I**) algorithm in SKCM-Metastasis.

3.4. Correlation between CYP1B1 and TMB, MSI and Neoantigen

To understand the role of CYP1B1 in immunotherapy, the association between CYP1B1 and immunotherapy-related biomarkers (TMB, MSI and neoantigen) was further assessed. As shown in Figure 4, CYP1B1 expression was positively associated with the TMB in COAD ($p = 0.0044$; Figure 4A) and LIHC ($p = 0.00011$; Figure 4A), and a negative association was found in STAD ($p = 0.038$; Figure 4A). CYP1B1 expression positively correlated significantly with MSI in OV ($p = 0.0019$) and LIHC ($p = 0.0038$) in Figure 4B, while a negative association in KIRP ($p = 0.03$), SARC ($p = 8.7 \times 10^{-5}$), STAD ($p = 0.0074$), SKCM ($p = 0.05$), CHOL ($p = 0.0032$) and HNSC ($p = 0.029$) was identified in Figure 4B. Similarly, CYP1B1 expression positively correlated significantly with neoantigen in LIHC ($p = 0.0012$) and READ ($p = 0.046$) in Figure 4C, while a negative association in STAD ($p = 0.037$) was revealed in Figure 4C. The results indicated that immunotherapy-related biomarkers mediated by CYP1B1 may play important roles in immune pathways. As the CYP1B1 was one of metabolic enzymes in melatonin, we further explored the melatonin-related pathways, including melatonin biosynthesis, circadian clock, entrainment of the circadian clock, entrainment of the circadian clock by photoperiod, and BMAL1_clock_NPAS2 circadian gene expression. As shown in Figure 4D and E, a high expression of CYP1B1 was associated with the inactivation of melatonin biosynthesis in LIHC ($p < 0.0001$) and STAD, associated with the activation of the circadian clock, entrainment of the circadian clock, entrainment of the circadian clock by photoperiod, and BMAL1_clock_NPAS2 circadian gene expression (Figure 4D,E). These results indicated that melatonin metabolism mediated by CYP1B1 may be involved in the complexity and heterogeneity of TME in cancer.

To further uncover the role of CYP1B1 in TME, 10 classical immune-related pathways, including immunological synapse, innate immune response, immunoglobulin complex, immunoglobulin binding, type 2 response, humoral immune response, immune effector process, B cell mediated immunity, adaptive immune response, and T cell mediated immunity, were enriched by ssGSEA analysis. Compared with low expression of CYP1B1, a high expression of CYP1B1 was significantly associated with the activation of immune-related pathways in LIHC (Figure 4F) and STAD (Figure 4G).

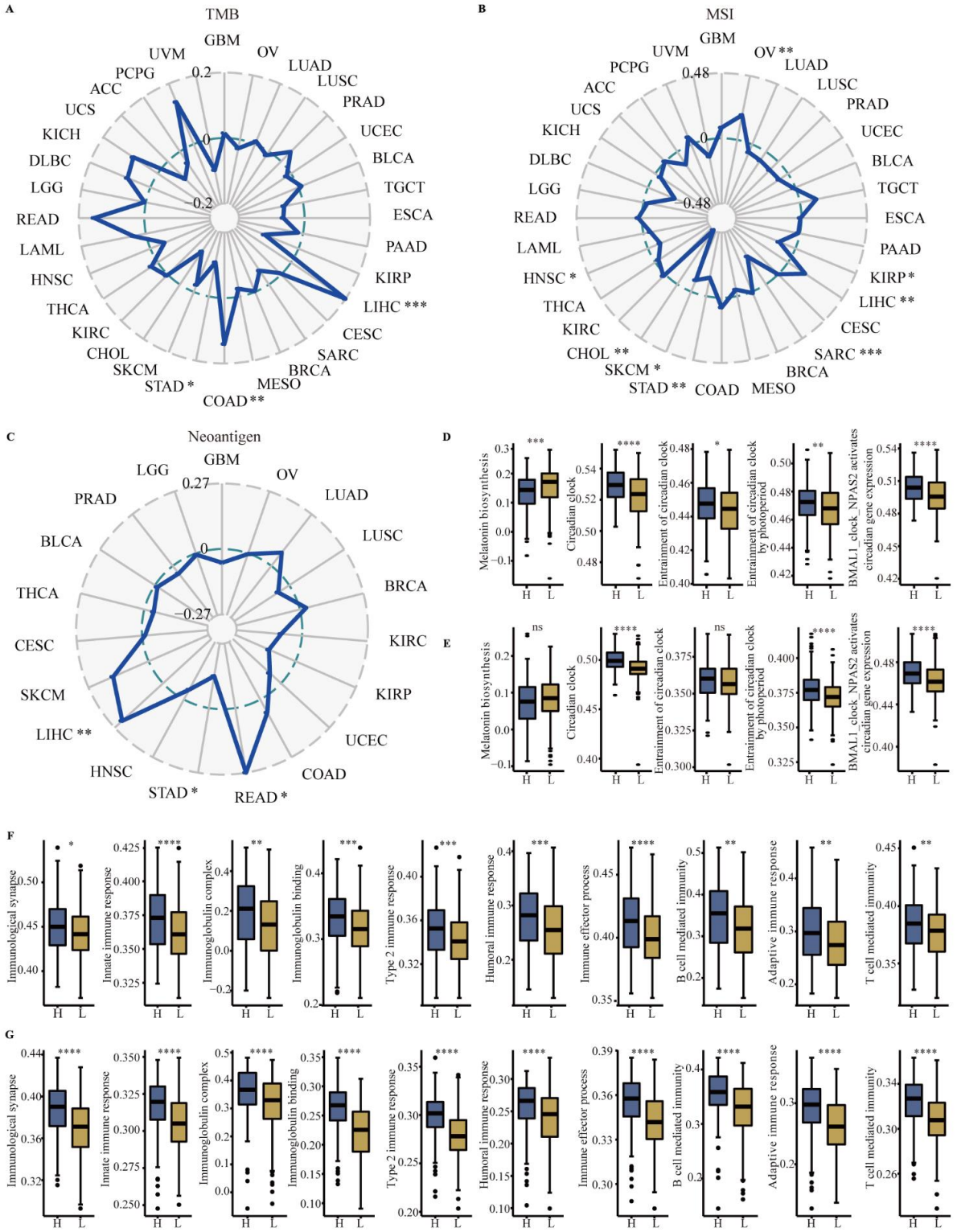

Figure 4. The correlations between CYP1B1 expression and TMB, MSI, neoantigen, and immune-related pathways. (**A**) Correlations between CYP1B1 expression and TMB in cancer. (**B**) Correlation between CYP1B1 and MSI in cancer. (**C**) Correlation between CYP1B1 and neoantigen in cancer. (**D**,**E**) The melatonin-related pathways enriched by ssGSEA analysis in LIHC (**D**) and STAD (**E**). (**F**,**G**) The classical immune related pathways enriched by ssGSEA analysis in LIHC (**F**) and STAD (**G**). Two groups (High-expression and Low-expression) of pathway scores with boxplots using the Mann-Whitney U test. * $p < 0.05$; ** $p < 0.01$; *** $p < 0.001$; **** $p < 0.0001$.

3.5. The Association of CYP1B1 Expression and Therapeutic Response

To identification the function of CYP1B1 in breast cancer, as shown in Figure 5A, GSEA analysis indicated that CYP1B1 was significantly associated with epithelial mesenchymal transition (NES = 2.625, FDR = 7.6×10^{-10}), angiogenesis (NES = 2.169, FDR = 9.2×10^{-6}), and regulation of the immune response (NES = 2.713, FDR = 3.1×10^{-9}) and circadian rhythm (NES = 0.822, FDR = 8.5×10^{-1}). Wound healing and transwell migration and invasion assays revealed that the overexpression CYP1B1 increased breast cancer migration and invasion (Figure 5B and C). Colony assays identified that CYP1B1 also improved breast cancer proliferation (Figure 5D). To explore the function of CYP1B1 in vivo, a tumor metastasis model was established and the immunohistochemical staining analysis of serial tissue sections showed that the expression of angiogenesis marker CD31, proliferation marker ki67, metastasis marker MMP9, and neutrophil infiltration marker LY6G mediated by CYP1B1 could be reversed by melatonin (Figure 6).

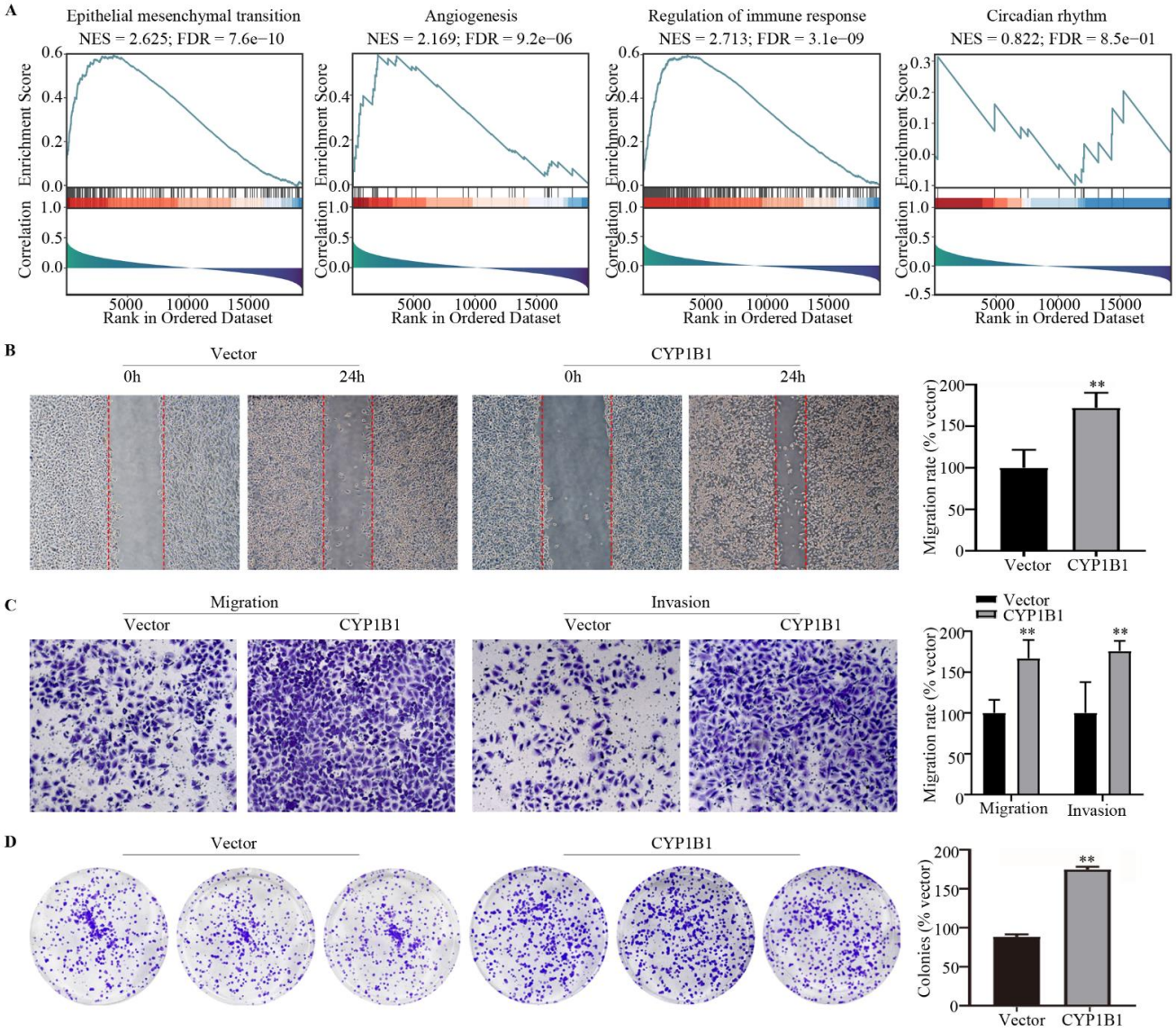

Figure 5. The function of CYP1B1 in vitro. (**A**) GSEA analysis of CYP1B1 in breast cancer. (**B**) Wound healing of CYP1B1. (**C**) Transwell migration and invasion assay of CYP1B1. (**D**) Colonies assay of CYP1B1. ** $p < 0.01$.

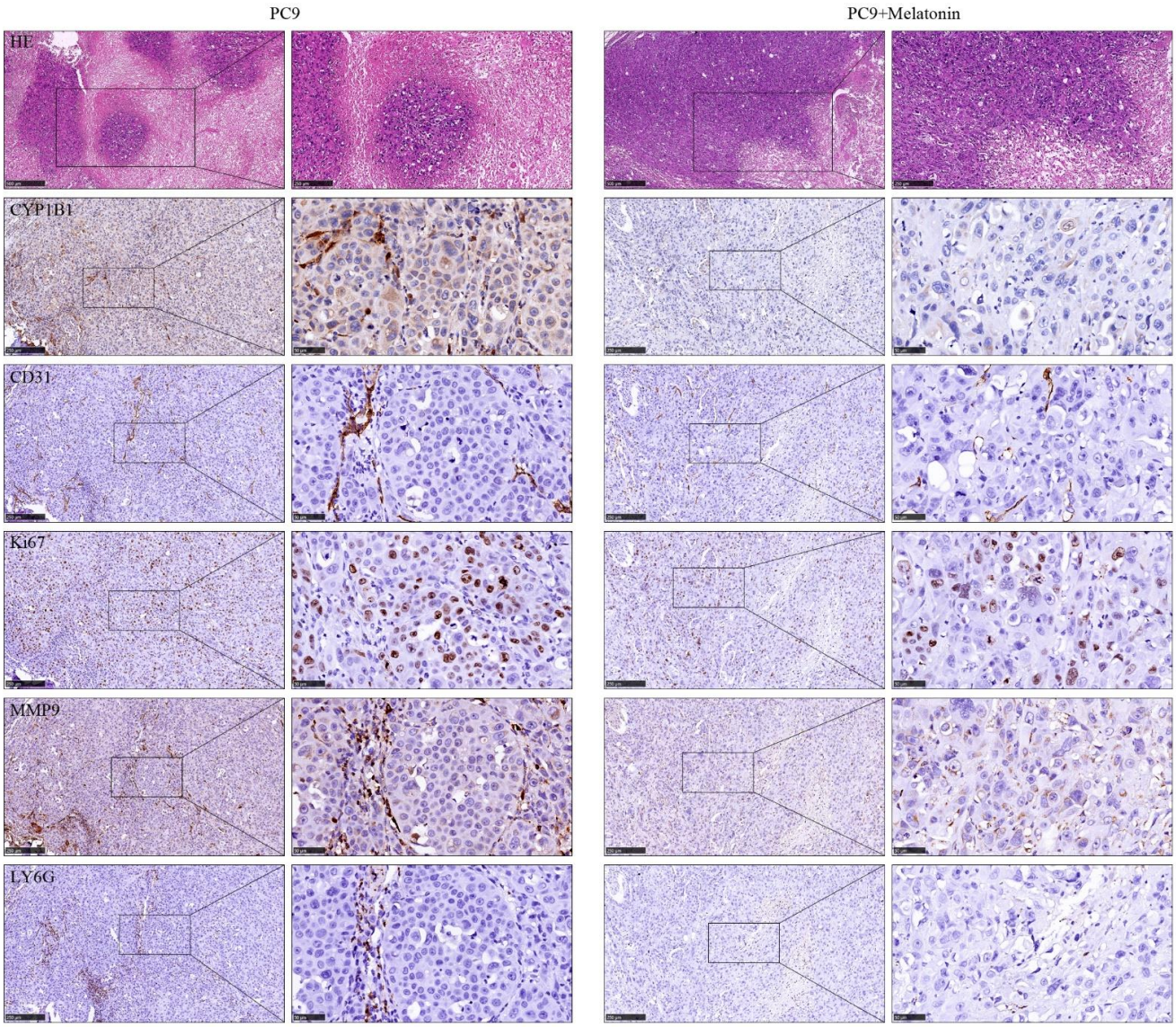

Figure 6. The HE and immunohistochemical staining of CD31, ki67, MMP9, and LY6G between PC9 and PC9 + Melatonin groups.

3.6. Identification of Immune Subtype, Molecular Subtype and Immune Response

The associations of CYP1B1 expression on immune and molecular subtypes in cancers was investigated. Overall, six immune subtypes, including wound healing (C1 subtype), IFN-γ dominant (C2 subtype), inflammatory (C3 subtype), lymphocyte depleted (C4 subtype), immunologically quiet (C5 subtype), and TGF-β dominant (C6 subtype) were analyzed. As depicted in Figure 7A, the expression of CYP1B1 was significantly associated with immune subtype in BRCA, CHOL, COAD, HNSC, KIRC, LGG, LIHC, LUAD, LUSC, PAAD, PCPG, PRAD, READ, SARC, STAD, THCA, UCEC, and UVM. The top eight immune subtypes, including BRCA ($p = 1.29 \times 10^{-12}$; Figure 7B), COAD ($p = 1.89 \times 10^{-6}$; Figure 7C), LGG ($p = 1.49 \times 10^{-5}$; Figure 7D), LUSC ($p = 3.28 \times 10^{-5}$; Figure 7E), PAAD ($p = 6.79 \times 10^{-7}$; Figure 7F), PCPG ($p = 2.52 \times 10^{-4}$; Figure 7G), STAD ($p = 6.93 \times 10^{-10}$; Figure 7H), and UVM ($p = 1.11 \times 10^{-5}$; Figure 7I), were revealed.

The associations between CYP1B1 expression and molecular subtypes were also significantly clarified in ACC, BRCA, COAD, ESCA, GBM, HNSC, KIRP, LGG, LUSC, OV, PCPG, PRAD, SKCM, and STAD. The top eight molecular subtypes, including BRCA ($p = 2.14 \times 10^{-11}$; Figure 7J), HNSC ($p = 6 \times 10^{-13}$; Figure 7K), LUSC ($p = 4.84 \times 10^{-13}$; Figure 7L), OV (p = 3.46e-10; Figure 7M), PCPG (p = 3.98e-05; Figure 7N), PRAD

($p = 1.11 \times 10^{-7}$; Figure 7O), SKCM ($p = 1.11 \times 10^{-7}$; Figure 7P), and STAD ($p = 5.21 \times 10^{-7}$; Figure 7Q), were also identified. These results indicated that the dysregulated expression of CYP1B1 was associated with different immune subtypes and molecular subtypes in cancer.

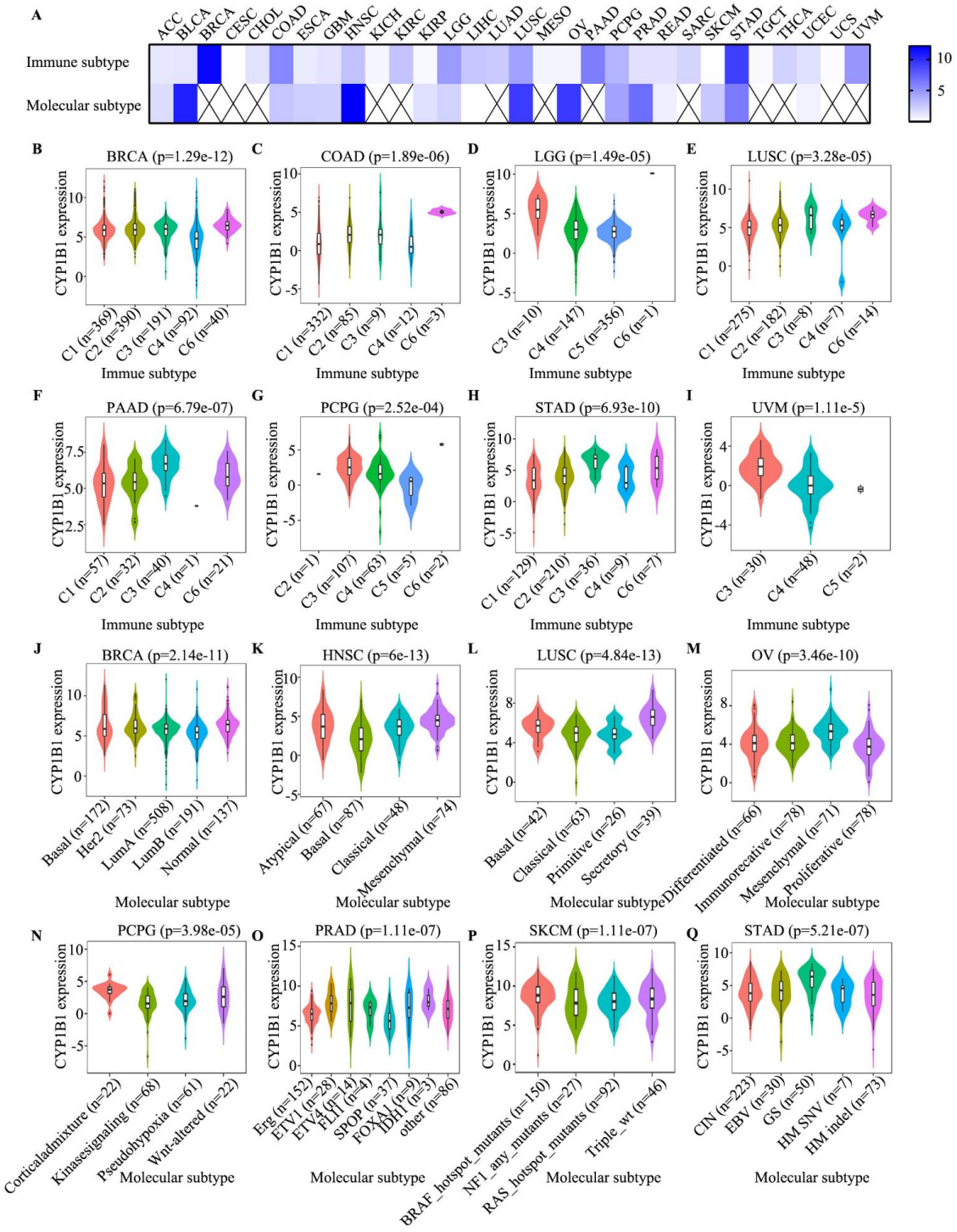

Figure 7. The associations between CYP1B1 expression and immune subtype and molecular subtype. (**A**) The heatmap of the Kruskal–Wallis test in the immune subtype and molecular subtype. (**B**–**I**) The top eight correlations between CYP1B1 expression and immune subtype in BRCA (**B**), COAD (**C**), LGG (**D**), LUSC (**E**), PAAD (**F**), PCPG (**G**), STAD (**H**), and UVM (**I**). (**J**–**Q**) The top eight correlations between CYP1B1 expression and molecular subtype in BRCA (**J**), HNSC (**K**), LUSC (**L**), OV (**M**), PCPG (**N**), PRAD (**O**), SKCM (**P**), and STAD (**Q**) (Kruskal–Wallis test, $p < 0.05$ was considered to be significant.).

To further reveal the clinical application of CYP1B1, we first evaluate the roles of CYP1B1 in GSE67501, GSE91061, GSE100797, GSE111636, GSE115821, GSE126044, GSE135222, GSE173839, IMvigor210, Nathanson cohort 2017, VanAllen cohort 2015, and immune cohorts. The predictive power of CYP1B1 was 0.679, 0.606, 0.596, 0.600, 0.608, 0.836, 0.579, 0.559, 0.564, 0.625, and 0.674, respectively, in anti-PD-1/PD-L1/CAR-T/CTLA4 cohorts (Figure 8). As shown in Figure S5, IC50 of HDAC, TOP1, RAF, c-MET, MEK, RAF, CDK4, ALK, RTK, GS, FGFR, and MDM2 inhibitor in high CYP1B1 expression was significantly upregulated, which indicated that CYP1B1 was associated with therapeutic resistance. However, the expression of CYP1B1 was also associated with the therapeutic sensitivity of AZD530 and erlotinib (Figure S5, $p < 0.05$). These results revealed that CYP1B1 may be a promising molecular target in clinical treatment.

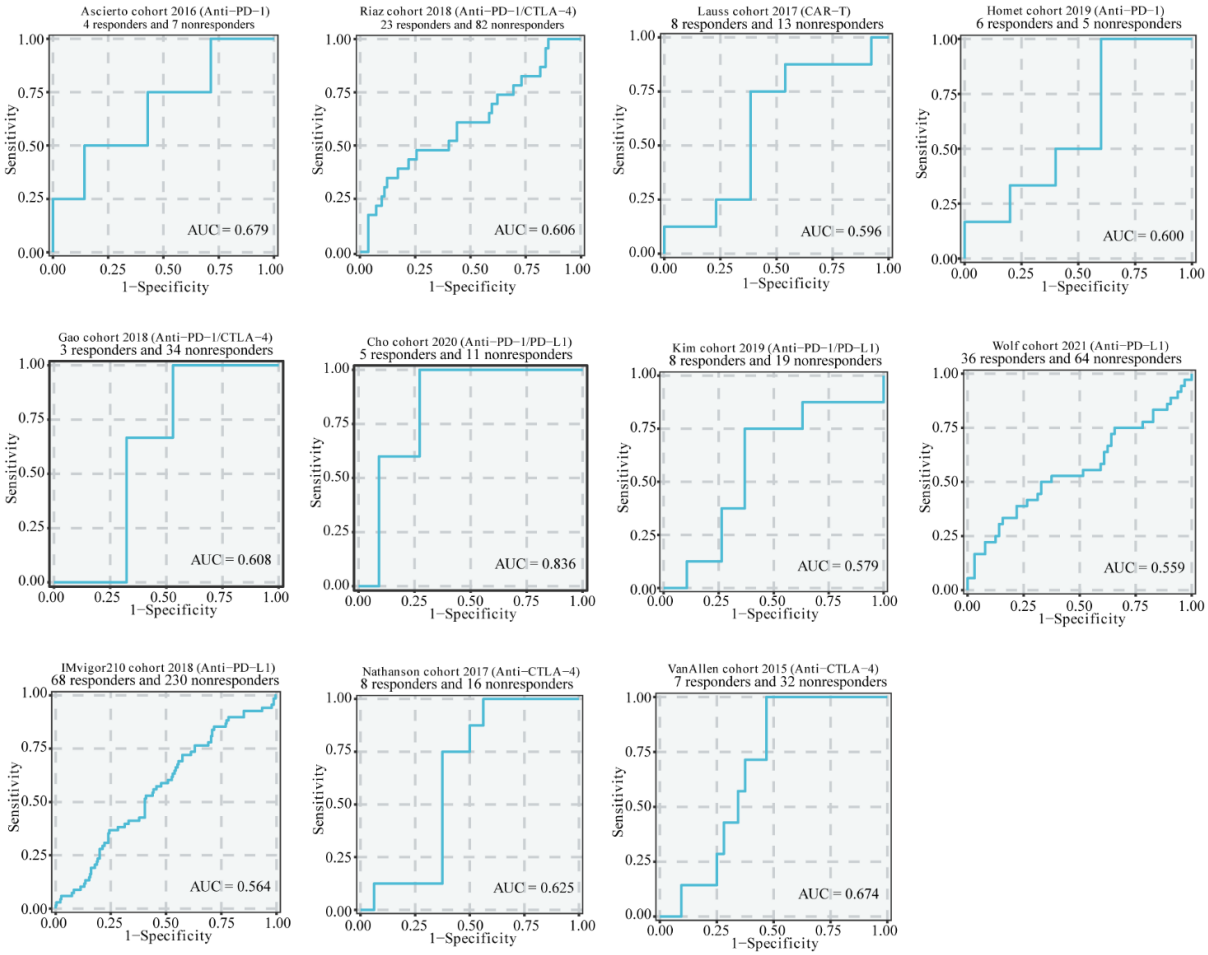

Figure 8. The predictive power of CYP1B1 in GSE67501, GSE91061, GSE100797, GSE111636, GSE115821, GSE126044, GSE135222, GSE173839, IMvigor210, Nathanson cohort 2017, VanAllen cohort 2015 immune cohorts.

4. Discussion

Melatonin has been considered a promising anti-cancer drug in the treatment of cancer [32–34]. However, the molecular and clinical characteristics of the melatonergic metabolic enzyme CYP1B1 in cancer still remain unknown. In this study, we comprehensively investigated the clinical and immunological pattern of CYP1B1 determined from RNA-seq data across TCGA pan-cancer. The results indicated that the dysregulated expression of CYP1B1 was correlated with clinical and immunological characteristics in cancer and could be a promising predictor and molecular target for clinical immune treatment.

CYP1B1, one member of the cytochrome P450 family, has been identified in tumorigenesis [35,36]. The dysregulated expression of CYP1B1 was explored between tumor

and normal tissues. As a result of the abnormal expression in cancer, CYP1B1 has been defined as a candidate tumor antigen [37]. Interestingly, CYP1B1 has also been exploited as a molecular target for immunotherapy, owing to the restricted expression profile in normal tissues [38]. Differential CYP1B1 expression was also observed in different clinical stages and tumor grades, and a high expression of CYP1B1 was also observed in renal cell carcinoma, which was related to advanced grades and late stages [39]. In vitro and vivo function experiments identified that CYP1B1 could increase tumor progression and metastasis. The results indicated that CYP1B1 was correlated with clinical characteristics in cancer and could be a prognostic predictor in cancer.

In the present study, the infiltration of lymphocyte, immune regulators, CAFs, immune subtype, and molecular subtype was mediated by CYP1B1. By using genetic study of the melatonergic microenvironment across 14 solid tumors, Lv et al. also identified that the melatonin catabolic enzymes, including CYP1B1, were associated with TMB and prognosis [40]. In vitro experiments found that the CYP1B1 expression was significantly correlated with B7-H3 expression in colorectal cancer. Nevertheless, in vivo experiments revealed that HLA-A*0201 could be processed and presented by CYP1B1-specific cytotoxic T lymphocytes (CTLs) [41,42]. The neutrophil infiltration mediated by CYP1B1 in the TME could be reversed by melatonin in vivo. Based on these findings, we speculated that CYP1B1 may regulate the immune cell infiltration in the tumor microenvironment, which could act as a molecular marker for clinical therapy.

TMB, MSI, and neoantigen have been identified as biomarkers for predicting the response of immune checkpoint inhibitors in cancer [43,44]. Our results found that CYP1B1 expression was associated with TMB, MSI, and neoantigen in pan-cancer, especially in LIHC and STAD. ssGESA analysis CYP1B1 was associated with melatonergic and immune-related pathways and therapeutic response. Recent studies showed that CYP1B1 was involved in the drug resistance of tumor cells, such as paclitaxel and docetaxel [45–47]. The clinical trial of CYP1B1-directed vaccination identified that patients with solid and hematologic tumors can benefit from anti-CYP1B1 immunity [48]. Thus, targeting CYP1B1 may be a useful way for the development of anticancer treatment.

However, several issues need to be further explored. First, the clinical and immunological characteristics of CYP1B1 in cancer were based on the public database; the roles of CYP1B1 still needs to be further verified by multi-center data. Second, the function of CYP1B1 has been clarified in vitro and vivo, but the function of CYP1B1 knock-down or its inhibition need to be further explored and the potential mechanism of CYP1B1 in TME remains unclear. Third, although the CYP1B1 has promising predictive power for ICI in 11 clinical cohorts, its predictive power still needs to be validated on a larger number of immune cohorts. Finally, the immunological CYP1B1 in pan-cancer needs additional investigation to clarify its function and processes.

5. Conclusions

In conclusion, we comprehensively analyzed the clinical and immunological characteristics of CYP1B1 across 33 solid tumors. Our results identified that the dysregulated expression of CYP1B1 was associated with the clinical stage, tumor grade, immune cell infiltration, TMB, MSI, neoantigen, activation of multiple melatonergic and immune-related pathways, and therapeutic resistance. Targeting CYP1B1 might be a promising predictor and molecular target for clinical treatment.

Supplementary Materials: The following supporting information can be downloaded at: https://www.mdpi.com/article/10.3390/cancers14225641/s1, Figure S1. Forest plots of CYP1B1 expression on the prognosis in cancer. (A) Effect of CYP1B1 on overall survival (OS) in cancer. (B) Effect of CYP1B1 on disease specific survival (DSS) in 33 types of cancers. (C) Effect of CYP1B1 on disease free interval (DFI) in cancer. (D) Effect of CYP1B1 on progression free interval (PFI) in cancer. The red line means risky factor in prognosis, the blue line means protective in prognosis, the grey line means no significance in prognosis. Figure S2. The negative correlation between CYP1B1 expression and tumor grade in LIHC. Figure S3. The correlations between CYP1B1 expression and immunomodulator. (A)

The spearman correlations between CYP1B1 expression and immunostimulator in cancer. (B) The spearman correlations between CYP1B1 expression and immunoinhibitor in cancer. The heatmap represents rho value. Red color means positive correlation, blue color means negative correlation. Four associations were showed by dot plots. Figure S4. The correlations between CYP1B1 expression and chemokine and receptor. (A) The spearman correlations between CYP1B1 expression and chemokine in cancer. (B) The spearman correlations between CYP1B1 expression and receptor in cancer. The heatmap represents rho value. Red color means positive correlation, blue color means negative correlation. Four associations were showed by dot plots. Figure S5. The IC50 between high and low CYP1B1 expression in normal tissue.

Author Contributions: B.Y.: Data curation, Formal analysis, Investigation; G.L.: Investigation, Resources, Software; Z.D.: Conceptualization, Data curation, Software; L.W.: Investigation, Supervision, Validation; B.L.: Methodology, Data curation, Visualization; J.Z.: Writing—original draft, Writing—review & editing. All authors have read and agreed to the published version of the manuscript.

Funding: This study was supported by grants from the National Natural Science Foundation of China (82003212), Science and Technology Program of Guangzhou (202201010970) and the Discipline Construction Project of Guangzhou Medical University during the 14th Five-Year Plan (06-410-2107181).

Institutional Review Board Statement: The study was conducted in accordance with the Declaration of Helsinki (as revised in 2013) and was approved by the Ethics Committee of The Sixth People's Hospital of Huizhou City (PJ2022MI-KJ038).

Informed Consent Statement: Not applicable.

Data Availability Statement: The data presented in this study are available in this article and Supplementary Material.

Acknowledgments: The authors would like to thank the staff members of the Cancer Genome Atlas for their involvement in the cBioPortal for Cancer Genomics Program.

Conflicts of Interest: The authors declare that they have no competing interest.

References

1. Brzezinski, A. Melatonin in humans. *N. Engl. J. Med.* **1997**, *336*, 186–195. [CrossRef]
2. Cagnacci, A. Melatonin in relation to physiology in adult humans. *J. Pineal Res.* **1996**, *21*, 200–213. [CrossRef] [PubMed]
3. Simonneaux, V.; Ribelayga, C. Generation of the melatonin endocrine message in mammals: A review of the complex regulation of melatonin synthesis by norepinephrine, peptides, and other pineal transmitters. *Pharmacol. Rev.* **2003**, *55*, 325–395. [CrossRef] [PubMed]
4. Ma, X.; Idle, J.R.; Krausz, K.W.; Gonzalez, F.J. Metabolism of melatonin by human cytochromes p450. *Drug Metab. Dispos.* **2005**, *33*, 489–494. [CrossRef] [PubMed]
5. Carstensen, M.B.; Medvetzky, A.; Weinberger, A.; Driever, W.; Gothilf, Y.; Rath, M.F. Genetic ablation of the Bsx homeodomain transcription factor in zebrafish: Impact on mature pineal gland morphology and circadian behavior. *J. Pineal Res.* **2022**, *72*, e12795. [CrossRef]
6. Kent, B.A.; Rahman, S.A.; St. Hilaire, M.A.; Grant, L.K.; Ruger, M.; Czeisler, C.A.; Lockley, S.W. Circadian lipid and hepatic protein rhythms shift with a phase response curve different than melatonin. *Nat. Commun.* **2022**, *13*, 681. [CrossRef]
7. Hartstein, L.E.; Behn, C.D.; Akacem, L.D.; Stack, N.; Wright, K.P., Jr.; Lebourgeois, M.K. High sensitivity of melatonin suppression response to evening light in preschool-aged children. *J. Pineal Res.* **2022**, *72*, e12780. [CrossRef]
8. Wang, L.; Wang, C.; Choi, W.S. Use of Melatonin in Cancer Treatment: Where Are We? *Int. J. Mol. Sci.* **2022**, *23*, 3779. [CrossRef]
9. Leelaviwat, N.; Mekraksakit, P.; Cross, K.M.; Landis, D.M.; Mclain, M.; Sehgal, L.; Payne, J.D. Melatonin: Translation of Ongoing Studies into Possible Therapeutic Applications Outside Sleep Disorders. *Clin. Ther.* **2022**, *44*, 783–812. [CrossRef]
10. Bantounou, M.; Plascevic, J.; Galley, H.F. Melatonin and Related Compounds: Antioxidant and Anti-Inflammatory Actions. *Antioxidants* **2022**, *11*, 532. [CrossRef]
11. Liu, S.C.; Tsai, C.H.; Wang, Y.H.; Su, C.M.; Wu, H.C.; Fong, Y.C.; Yang, S.F.; Tang, C.H. Melatonin abolished proinflammatory factor expression and antagonized osteoarthritis progression in vivo. *Cell Death Dis.* **2022**, *13*, 215. [CrossRef] [PubMed]
12. Zeng, L.; He, J.; Liu, C.; Zhang, F.; Zhang, Z.; Chen, H.; Wang, Q.; Ding, X.; Luo, H. Melatonin Attenuates Ropivacaine-Induced Apoptosis by Inhibiting Excessive Mitophagy Through the Parkin/PINK1 Pathway in PC12 and HT22 Cells. *Inflammation* **2022**, *45*, 725–738. [CrossRef] [PubMed]
13. Luo, X.; Chen, Y.; Tang, H.; Wang, H.; Jiang, E.; Shao, Z.; Liu, K.; Zhou, X.; Shang, Z. Melatonin Inhibits EMT and PD-L1 Expression through the ERK1/2/FOSL1 Pathway and Regulates Anti-Tumor Immunity in HNSCC. *Cancer Sci.* **2022**, *113*, 2232–2245. [CrossRef] [PubMed]

14. Guo, J.; Bai, Y.; Wei, Y.; Dong, Y.; Zeng, H.; Reiter, R.J.; Shi, H. Fine-tuning of pathogenesis-related protein 1 (PR1) activity by the melatonin biosynthetic enzyme ASMT2 in defense response to cassava bacterial blight. *J. Pineal Res.* **2022**, *72*, e12784. [CrossRef] [PubMed]
15. Li, M.; Hao, B.; Zhang, M.; Reiter, R.J.; Lin, S.; Zheng, T.; Chen, X.; Ren, Y.; Yue, L.; Abay, B. Melatonin enhances radiofrequency-induced NK antitumor immunity, causing cancer metabolism reprogramming and inhibition of multiple pulmonary tumor development. *Signal Transduct. Target. Ther.* **2021**, *6*, 330. [CrossRef] [PubMed]
16. Wang, Y.; Tao, B.; Li, J.; Mao, X.; He, W.; Chen, Q. Melatonin Inhibits the Progression of Oral Squamous Cell Carcinoma via Inducing miR-25-5p Expression by Directly Targeting NEDD9. *Front. Oncol.* **2020**, *10*, 543591. [CrossRef]
17. Chuffa, L.G.D.A.; Carvalho, R.F.; Justulin, L.A.; Cury, S.S.; Seiva, F.R.F.; Jardim-Perassi, B.V.; de Campos Zuccari, D.A.P.; Reiter, R.J. A meta-analysis of microRNA networks regulated by melatonin in cancer: Portrait of potential candidates for breast cancer treatment. *J. Pineal Res.* **2020**, *69*, e12693. [CrossRef]
18. Fathizadeh, H.; Mirzaei, H.; Asemi, Z. Melatonin: An anti-tumor agent for osteosarcoma. *Cancer Cell Int.* **2019**, *19*, 319. [CrossRef]
19. Ross, J. Comments on the article "Persistent confusion of total entropy and chemical system entropy in chemical thermodynamics" [(1996) *Proc. Natl. Acad. Sci. USA* 93,7452–7453]. *Proc. Natl. Acad. Sci. USA* **1996**, *93*, 14314; discussion 14315. [CrossRef]
20. Crewe, H.K.; Notley, L.M.; Wunsch, R.M.; Lennard, M.S.; Gillam, E.M.J. Metabolism of tamoxifen by recombinant human cytochrome P450 enzymes: Formation of the 4-hydroxy, 4′-hydroxy and N-desmethyl metabolites and isomerization of trans-4-hydroxytamoxifen. *Drug Metab. Dispos.* **2002**, *30*, 869–874. [CrossRef]
21. Shou, M.; Korzekwa, K.R.; Krausz, K.W.; Buters, J.T.; Grogan, J.; Goldfarb, I.; Hardwick, J.P.; Gonzalez, F.J.; Gelboin, H.V. Specificity of cDNA-expressed human and rodent cytochrome P450s in the oxidative metabolism of the potent carcinogen 7,12-dimethylbenz[a]anthracene. *Mol. Carcinog.* **1996**, *17*, 241–249. [CrossRef]
22. Shimada, T.; Gillam, E.M.; Sutter, T.R.; Strickland, P.T.; Guengerich, F.P.; Yamazaki, H. Oxidation of xenobiotics by recombinant human cytochrome P450 1B1. *Drug Metab. Dispos.* **1997**, *25*, 617–622. [PubMed]
23. Tanaka, Y.; Sasaki, M.; Kaneuchi, M.; Shiina, H.; Lgawa, M.; Dahiya, R. Polymorphisms of the CYP1B1 gene have higher risk for prostate cancer. *Biochem. Biophys. Res. Commun.* **2002**, *296*, 820–826. [CrossRef]
24. Mcgrath., M.; Hankinson, S.E.; Arbeitman, L.; Colditz, G.A.; Hunter, D.J.; Vivo, I.D. Cytochrome P450 1B1 and catechol-O-methyltransferase polymorphisms and endometrial cancer susceptibility. *Carcinogenesis* **2004**, *25*, 559–565. [CrossRef] [PubMed]
25. Li, C.; Long, B.; Qin, X.; Li, W.; Zhou, Y. Cytochrome P1B1 (CYP1B1) polymorphisms and cancer risk: A meta-analysis of 52 studies. *Toxicology* **2015**, *327*, 77–86. [CrossRef]
26. Mohamed, H.T.; Gadalla, R.; El-husseiny, N.; Hassan, H.; Wang, Z.; Ibrahim, S.A.; EI-Shinawi, M.; Sherr, D.H.; Mohamed, M.M. Inflammatory breast cancer: Activation of the aryl hydrocarbon receptor and its target CYP1B1 correlates closely with Wnt5a/b-beta-catenin signalling, the stem cell phenotype and disease progression. *J. Adv. Res.* **2019**, *16*, 75–86. [CrossRef] [PubMed]
27. Kwon, Y.J.; Baek, H.S.; Ye, D.J.; Shin, S.; Kim, D.; Chun, Y.J. CYP1B1 Enhances Cell Proliferation and Metastasis through Induction of EMT and Activation of Wnt/beta-Catenin Signaling via Sp1 Upregulation. *PLoS ONE* **2016**, *11*, e0151598. [CrossRef]
28. D'uva, G.; Baci, D.; Albini, A.; Noonan, D.M. Cancer chemoprevention revisited: Cytochrome P450 family 1B1 as a target in the tumor and the microenvironment. *Cancer Treat. Rev.* **2018**, *63*, 1–18. [CrossRef]
29. Hu, B.; Wu, C.; Mao, H.; Gu, H.; Dong, H.; Yan, J.; Qi, Z.; Yuan, L.; Dong, Q.; Long, J. Subpopulations of cancer-associated fibroblasts link the prognosis and metabolic features of pancreatic ductal adenocarcinoma. *Ann. Transl. Med.* **2022**, *10*, 262. [CrossRef]
30. Saw, P.E.; Chen, J.; Song, E. Targeting CAFs to overcome anticancer therapeutic resistance. *Trends Cancer* **2022**, *8*, 527–555. [CrossRef]
31. Ganguly, K.; Shah, A.; Atri, P.; Rauth, S.; Ponnusamy, M.P.; Kumar, S.; Batra, S.K. Chemokine-mucinome interplay in shaping the heterogeneous tumor microenvironment of pancreatic cancer. *Semin. Cancer Biol.* **2022**, *86*, 511–520. [CrossRef] [PubMed]
32. Zhang, J.; Jiang, H.; Du, K.; Xie, T.; Wang, B.; Chen, C.; Reiter, R.J.; Cen, B.; Yuan, Y. Pan-cancer analyses reveal genomics and clinical characteristics of the melatonergic regulators in cancer. *J. Pineal Res.* **2021**, *71*, e12758. [CrossRef] [PubMed]
33. Shin, Y.Y.; Seo, Y.; Oh, S.J.; Ahn, J.S.; Song, M.H.; Kang, M.J.; Oh, J.M.; Lee, D.; Kim, Y.H.; Sung, E.S.; et al. Melatonin and verteporfin synergistically suppress the growth and stemness of head and neck squamous cell carcinoma through the regulation of mitochondrial dynamics. *J. Pineal Res.* **2022**, *72*, e12779. [CrossRef] [PubMed]
34. Bilska, B.; Schedel, F.; Piotrowska, A.; Stefan, J.; Zmijewski, M.; Pyza, E.; Reiter, R.J.; Steinbrink, K.; Slominski, A.T.; Tulic, M.K.; et al. Mitochondrial function is controlled by melatonin and its metabolites in vitro in human melanoma cells. *J. Pineal Res.* **2021**, *70*, e12728. [CrossRef]
35. Kaminsky, L.S.; Spivack, S.D. Cytochromes P450 and cancer. *Mol. Aspects Med.* **1999**, *20*, 70–84, 137. [PubMed]
36. Silvestri, L.; Sonzogni, L.; De Silvestri, A.; Gritti, C.; Foti, L.; Zavaglia, C.; Leveri, M.; Cividini, A.; Mondelli, M.U.; Civardi, E.; et al. CYP enzyme polymorphisms and susceptibility to HCV-related chronic liver disease and liver cancer. *Int. J. Cancer* **2003**, *104*, 310–317. [CrossRef]
37. Murray, G.I.; Taylor, M.C.; Mcfadyen, M.C.; McKay, J.A.; Greenlee, W.F.; Burke, M.D.; Melvin, W.T. Tumor-specific expression of cytochrome P450 CYP1B1. *Cancer Res.* **1997**, *57*, 3026–3031. [PubMed]

38. Luby, T.M.; Cole, G.; Baker, L.; Kornher, J.S.; Ramstedt, U.; Hedley, M.L. Repeated immunization with plasmid DNA formulated in poly(lactide-co-glycolide) microparticles is well tolerated and stimulates durable T cell responses to the tumor-associated antigen cytochrome P450 1B1. *Clin. Immunol.* **2004**, *112*, 45–53. [CrossRef]
39. Mitsui, Y.; Chang, I.; Fukuhara, S.; Hiraki, M.; Arichi, N.; Yasumoto, H.; Hirata, H.; Yamamura, S.; Shahryari, V.; Deng, G.; et al. CYP1B1 promotes tumorigenesis via altered expression of CDC20 and DAPK1 genes in renal cell carcinoma. *BMC Cancer* **2015**, *15*, 942. [CrossRef]
40. Lv, J.W.; Zheng, Z.Q.; Wang, Z.X.; Zhou, G.Q.; Chen, L.; Mao, Y.P.; Lin, A.H.; Reiter, R.J.; Ma, J.; Chen, Y.P.; et al. Pan-cancer genomic analyses reveal prognostic and immunogenic features of the tumor melatonergic microenvironment across 14 solid cancer types. *J. Pineal Res.* **2019**, *66*, e12557. [CrossRef]
41. Maecker, B.; Sherr, D.H.; Vonderheide, R.H.; von Bergwelt-Baildon, M.S.; Hirano, N.; Anderson, K.S.; Xia, Z.; Butler, M.O.; Wucherpfennig, K.W.; O'Hara, C.; et al. The shared tumor-associated antigen cytochrome P450 1B1 is recognized by specific cytotoxic T cells. *Blood* **2003**, *102*, 3287–3294. [CrossRef] [PubMed]
42. Maecker, B.; von Bergwelt-Baildon, M.S.; SHERR, D.H.; Nadler, L.M.; Schultze, J.L. Identification of a new HLA-A*0201-restricted cryptic epitope from CYP1B1. *Int. J. Cancer.* **2005**, *115*, 333–336. [CrossRef] [PubMed]
43. Duffy, M.J. Crown J Biomarkers for Predicting Response to Immunotherapy with Immune Checkpoint Inhibitors in Cancer Patients. *Clin. Chem.* **2019**, *65*, 1228–1238. [CrossRef] [PubMed]
44. Nagaoka, K.; Sun, C.; Kobayashi, Y.; Kanaseki, T.; Tokita, S.; Komatsu, T.; Maejima, K.; Futami, J.; Nomura, S.; Udaka, K.; et al. Identification of Neoantigens in Two Murine Gastric Cancer Cell Lines Leading to the Neoantigen-Based Immunotherapy. *Cancers* **2021**, *14*, 106. [CrossRef] [PubMed]
45. Zhu, Z.; Mu, Y.; Qi, C.; Wang, J.; Xi, G.; Guo, J.; Mi, R.; Zhao, F. CYP1B1 enhances the resistance of epithelial ovarian cancer cells to paclitaxel in vivo and in vitro. *Int. J. Mol. Med.* **2015**, *35*, 340–348. [CrossRef]
46. Chen, P.; Wang, S.; Cao, C.; Ye, W.; Wang, M.; Zhou, C.; Chen, W.; Zhang, X.; Zhang, K.; Zhou, W. alpha-naphthoflavone-derived cytochrome P450 (CYP)1B1 degraders specific for sensitizing CYP1B1-mediated drug resistance to prostate cancer DU145: Structure activity relationship. *Bioorg. Chem.* **2021**, *116*, 105295. [CrossRef]
47. Lin, Q.; Cao, J.; Du, X.; Yang, K.; Yang, X.; Liang, Z.; Shi, J.; Zhang, J. CYP1B1-catalyzed 4-OHE2 promotes the castration resistance of prostate cancer stem cells by estrogen receptor alpha-mediated IL6 activation. *Cell Commun. Signal.* **2022**, *20*, 31. [CrossRef]
48. Gribben, J.G.; Ryan, D.P.; Boyajian, R.; Urban, R.G.; Hedley, M.L.; Beach, K.; Nealon, P.; Matulonis, U.; Campos, S.; Gilligan, T.D.; et al. Unexpected association between induction of immunity to the universal tumor antigen CYP1B1 and response to next therapy. *Clin. Cancer Res.* **2005**, *11*, 4430–4436. [CrossRef]